UC Berkeley
UC Berkeley Previously Published Works

Title

Forest responses to simulated elevated CO2 under alternate hypotheses of size- and age-dependent mortality

Permalink

Journal

ISSN

Authors

Needham, Jessica F
Chambers, Jeffrey
Fisher, Rosie
et al.

Publication Date

DOI

Peer reviewed

Forest responses to simulated elevated CO_2 under alternate hypotheses of size- and age-dependent mortality

Jessica F. Needham[1], Jeffrey Chambers[1], Rosie Fisher[2], Ryan Knox[1], and Charles D. Koven[1]

[1]Climate and Ecosystem Sciences Department, Lawrence Berkeley National Laboratory, Berkeley, CA, USA

[2]Centre Européen de Recherche et de Formation Avancée en Calcul Scientifique, Toulouse, France

1

Abstract

Elevated atmospheric carbon dioxide (eCO_2) is predicted to increase growth rates of forest trees. The extent to which increased growth translates to changes in biomass is dependent on the turnover time of the carbon, and thus tree mortality rates. Size- or age- dependent mortality combined with increased growth rates could result in either decreased carbon turnover from a speeding up of tree life cycles, or increased biomass from trees reaching larger sizes, respectively. However, most vegetation models currently lack any representation of size- or age-dependent mortality and the effect of eCO_2 on changes in biomass and carbon turnover times is thus a major source of uncertainty in predictions of future vegetation dynamics. Using a reduced-complexity form of the dynamic vegetation model FATES to simulate an idealised tropical forest, we find increases in biomass despite reductions in carbon turnover time in both size- and age-dependent mortality scenarios in response to a hypothetical eCO_2-driven 25% increase in NPP. Carbon turnover times decreased by 9.6% in size-dependent mortality scenarios due to a speeding up of tree life cycles, but also by 2.0% when mortality was age-dependent, as larger crowns led to increased light competition. Increases in AGB were much larger when mortality was age-dependent (24.3%) compared with size-dependent (13.4%) as trees reached larger sizes before death. In simulations with a constant background mortality rate, carbon turnover time decreased by 2.1% and AGB increased by 24.0%, however, absolute values of AGB and carbon turnover were higher than in either size- or age-dependent mortality scenario. The extent to which AGB increases and carbon turnover decreases will thus depend on the mechanisms of large tree mortality: if increased size itself results in elevated mortality rates, then this could reduce by about half the increase in AGB relative to the increase in woody NPP.

Keywords Vegetation models, carbon turnover times, forest dynamics, tree mortality, CO_2 fertilisation, global change

2

1 Introduction

Anthropogenic carbon emissions are causing atmospheric carbon dioxide (CO_2) to rise, leading to an increase in leaf-level photosynthesis (Herrick & Thomas, 1999), and a subsequent increase in individual-level plant growth rates (Ainsworth & Long, 2005). CO_2 fertilisation of plant growth is thought to explain much of the terrestrial carbon sequestration over recent decades (Sitch *et al.*, 2015), as well as observed increases in global leaf area index (Zhu *et al.*, 2016). However, significant uncertainty remains regarding the affect of eCO_2 on ecosystem level carbon uptake and carbon residence time (Arora *et al.*, 2019).

Free Air CO_2 Enrichment (FACE) experiments have followed the growth response of multiple terrestrial ecosystems to elevated CO_2. Although vegetation response to eCO_2 have differed between sites and through time, an initial increase in NPP of 25% was observed in two temperate forest FACE experiments following an increase in CO_2 by approximately 150 - 200 µmol mol^{-1} (Zaehle *et al.*, 2014). However, The FACE experiments were not designed to test the effect of eCO_2 on mortality or carbon residence times, and their relatively short time-scales make it impossible to draw conclusions regarding long-term shifts in carbon sequestration.

Large trees uptake and store the majority of aboveground forest carbon (Stephenson *et al.*, 2014), contribute disproportionately to reproduction (Fonseca *et al.*, 2009; Naito *et al.*, 2008) and define the physical structure of the forest, thus determining light levels to the understory below (Canham *et al.*, 1994). The dynamics of large trees are therefore critical to accurately representing forests and the exchange of carbon between the land and atmosphere in Earth system models (ESMs).

A 'U' shaped size-dependent mortality curve, with higher mortality rates in very small/young and very large/old trees, has been documented in a number of systems both tropical and temperate e.g. (Metcalf *et al.*, 2009; Lines *et al.*, 2010; Rüger *et al.*, 2011; Gonzalez-Akre *et al.*, 2016). Deconvolving the effects of increasing size and age on mortality is difficult (Vilalta, 2005; Mencuccini *et al.*, 2007) and little is known about how the interaction between growth and mortality rates at the individual level could influence the ecosystem-scale response to eCO_2 (Körner, 2017). ESMs typically do not represent either size- or age-dependant tree mortality as part of their representation of the terrestrial carbon cycle (e.g. (McDowell *et al.*, 2011; Bugmann *et al.*, 2019)). Within the minority of models which do consider this phenomena (e.g. (Arora & Boer, 2006)) the impacts of this representation have not been systematically assessed.

An increase in mortality rates of larger trees could result from the physical constraints on height imposed by hydraulic limitations (Koch *et al.*, 2004), with a resulting possible increased risk of drought (Nepstad *et al.*, 2007; da Costa *et al.*, 2010; Bennett *et al.*, 2015; McDowell & Allen, 2015), lightning strikes (Yanoviak *et al.*, 2015) or wind damage with size (Yap *et al.*, 2016).

Age-related changes to tree mortality risk remain poorly understood. Many features of plant architecture and physiology appear to limit the effects of senescence relative to animals. For example, meristem totipotency allows for continuous growth and production of new organs, a modular structure limits damage from somatic mutations, and high expression of resistance associated genes reduces the impact of pathogens (Klimešová *et al.*, 2015; Wang *et al.*, 2020). Experimental work suggests that size, rather than age-related cellular senescence, leads to decreases in net assimilation rates (Mencuccini *et al.*, 2005). However, an accumulation of physical damage through time could drive increased risk of mortality with age. The degree of crown damage or die-back, for example, was found to be a major determinant of the death of trees in a Bornean rainforest (Arellano *et al.*, 2019). Likewise, (Heineman *et al.*, 2015) found that over 50% of large trees from two sites in Borneo were infected with fungal heart rot. Although heart rot was associated with tree size (due to the relative ease of measuring size compared with age), it is likely that frequency and severity of pathogen infection correlates more strongly with age than with size. Thus, while it may be less likely that age is a strong contributor to increased large-tree mortality rates, we consider the possibility, and its resulting consequences, here.

If the probability of mortality of individual trees is primarily age-dependent, we would expect that increased growth rates following eCO_2 would allow trees to reach larger sizes before death, resulting in increased forest biomass with little change to turnover times. In contrast, if mortality probability is primarily size-dependent, we would expect increased growth rates to result in individuals moving through their life cycles more quickly, resulting in a decrease in vegetation carbon turnover time, and thus little change to biomass. Changes in carbon residence time have been identified as a major source of uncertainty in predictions of future forest dynamics (Friend *et al.*, 2014; Koven *et al.*, 2015b,a; Yu *et al.*, 2019; Pugh *et al.*, 2020). Quantifying the effects of size- versus age-dependent mortality, and identifying underlying mechanisms, is therefore a priority for identifying potential ecosystem responses to eCO_2 (McDowell *et al.*, 2018).

Most ESMs lack explicit representation of tree sizes and ages, and thus either size- or

4

age-dependent mortality (e.g. (McDowell *et al.*, 2011; Bugmann *et al.*, 2019)). Typically, mortality is modelled by a combination of mechanistic processes such as responses to productivity rates or carbon storage, wind damage (Lagergren *et al.*, 2012) and herbivory (Pachzelt *et al.*, 2015), along with a background mortality term that accounts for all other sources of mortality. Models that do include an age-related mortality term usually treat it similarly to the background mortality term - i.e. it is fixed rate across the life cycle that results in a specified fraction of the population exceeding some age limit (e.g. (Arora *et al.*, 2019)). Thus it does not explicitly model an increase in mortality risk at older ages or sizes. ESMs with neither size nor age dependent mortality thus implicitly assume that, all else being equal, an increase in productivity in response to eCO_2 will allow trees to reach larger sizes, thus increasing forest biomass. However a growth-longevity trade-off has been documented both within (Bigler & Veblen, 2009; Bugmann & Bigler, 2011; Büntgen *et al.*, 2019), and between species (Wright *et al.*, 2010), while observed changes in biomass and mortality across the Amazon suggests a recent speeding up of tree life cycles (Brienen *et al.*, 2015).

Lastly, ESMs typically do not include successional variation in their plant functional types (PFTs), instead defining PFTs based on biomes, gross plant morphology, and leaf morphology. However, successional variation is a key axis of plant variation within any biome, particularly for turnover times, as early successional trees tend to grow and die faster than late successional trees, and the successional balance within an ecosystem may be sensitive to changes in growth and mortality rates and thus CO_2 fertilisation (Laurance *et al.*, 2004).

Here we use a reduced-complexity configuration of a vegetation demographics model, the Functionally Assembled Terrestrial Ecosystem Simulator (FATES), to test alternate hypotheses of large-tree mortality: that mortality remains fixed at background levels, that it increases with plant size, and that it increases with plant age. We tested the response of ecosystem AGB and carbon turnover time to elevated NPP (eNPP) under each mortality scenario, compared to matched controls with constant NPP. Since we hypothesise that cohorts would reach larger sizes when mortality is age-dependent, we expected that results would be sensitive to allometric scaling. Likewise, we hypothesised that following an increase in NPP, size-dependent mortality would lead to an increase in the frequency of gap formation due to a speeding up of the life cycle and results would therefore be sensitive to parameters affecting canopy organisation. We tested the sensitivity of size- and age-dependent mortality simulations to allometric equations, specifically the scaling of DBH to height, AGB and

5

crown area.

Our initial tests were with one plant functional type (PFT). To test how the ecosystem response to eNPP changes with a range of plant functional strategies, we ran ensemble simulations in which two PFTs were parameterised with a range of observed growth and survival rates. We explored how the position of PFTs in this 'demographic' space altered co-existence and the response to eNPP.

2 Methods

2.1 Model description

FATES is a size- and age-structured vegetation model that tracks the state of cohorts: groups of trees of the same size and PFT modelled as one representative individual. Cohort dynamics are governed by physiological processes that depend on the interaction between functional traits and environmental drivers. FATES combines the Ecosystem Demography (ED) (Moorcroft *et al.*, 2001) approach to scaling from individuals to landscapes with elements of the Perfect Plasticity Approximation (PPA) approach to representing canopy organisation (Purves *et al.*, 2008; Fisher *et al.*, 2010). FATES must be run with a 'host' land model. At present, host models include the Community Land Model CLM (Lawrence *et al.*, 2019) or the Energy Exascale Earth System Model (E3SM) Land Model (ELM) (E3SM Project, 2018). The first combination of ED, PPA and CLM, was described in (Fisher *et al.*, 2015). PPA and ED are described in (Fisher *et al.*, 2018), initial sensitivity analysis at (Massoud *et al.*, 2019) and more recent FATES developments and benchmarking in (Koven *et al.*, 2019). Code is available at `https://github.com/NGEET/fates/`.

For this analysis we ran FATES in a novel 'prescribed physiology mode', a reduced complexity configuration that bypasses many of the physiological mechanisms of the model, following the modular complexity approach to land surface model design described in Fisher & Koven (2020). In the full FATES model, plant productivity is the result of a cascade of processes including light interception, photosynthesis, stomatal conductance, surface energy balance and plant respiration. To focus analysis on the dynamics of plant growth, canopy structure and mortality processes, in the prescribed physiology mode, both net primary productivity (NPP), as daily net productivity per unit crown area (kgC m^{-2} yr^{-1}), and background mortality rate become model parameters. Crown area is used to scale NPP to individual plants, as crown area determines the total area available for light interception, and

6

approximates the tree-to-forest scaling inherent in the PPA. Both these cohort-level inputs are dependant upon only PFT and canopy status (understory or canopy). Recruitment rates are also prescribed. Thus this mode requires five parameters to be specified per PFT instead of the full physiological model: canopy growth rate, understory growth rate, canopy mortality rate, understory mortality rate, and recruitment rate. We set leaf and root longevity to an arbitrary very large number so that allocation to meet demand from leaf and root turnover is essentially zero, thus allowing nearly all NPP to be allocated to structural growth each day. Thus the NPP and eNPP numbers we use are most analogous to woody NPP. This model configuration allows us to vastly reduce the dimensionality of parameter uncertainty from the many plant traits that regulate growth and mortality, to the growth and mortality rates themselves.

The prescribed physiology functionality can be thought of as an intermediate state on a spectrum of complexity, with end members defined by the full FATES model, and the ED and PPA analytic solutions described by (Farrior *et al.*, 2016). Farrior *et al.* (2016) re-create forest size structure by approximating canopy dynamics following disturbances. By defining woody mass growth increment as being constant per unit crown area, prescribed physiology mode is the minimally complex configuration that allows analyses in units of both individuals (as in (Farrior *et al.*, 2016)) and carbon (as in FATES).

In our simulations, tree mortality can have four causes: i) the prescribed background mortality rate, ii) either size- or age-dependent mortality rates that affect large or old cohorts, iii) impact mortality which kills small cohorts following gap creation, iv) and termination mortality that arises when the number of individuals in a cohort becomes so low as to cause numeric instability. Of these, only the size- and age-dependent rates are newly introduced here.

2.2 Model experiments

Our model experiments can be thought of as simulating an idealised tropical forest, since in prescribed physiology mode demographic rates are model parameters that are independent of climate driving data and site conditions.

All simulations were initiated with 1.3 m tall cohorts (corresponding to a DBH of 0.4 cm), at a density of 0.3 saplings per m^2. Simulations were run for 800 years in total, with a spin up of 300 years to reach equilibrium before the increase in NPP.

2.2.1 Simulated eNPP

To simulate an idealized case of elevated growth in response to eCO_2, we increased NPP by 25% over a period of approximately 100 years. We chose to use the value of a 25% increase in NPP to match FACE experiments where an increase in CO_2 from ambient (approximately 450 μmol mol^{-1}) to 537 - 550 μmol mol^{-1} increased NPP by approximately 25% at both the ORNL and Duke sites (Hendrey *et al.*, 1999; Norby *et al.*, 2002). We acknowledge that there is an additional component of uncertainty regarding the change in woody NPP relative to the change in total plant NPP (Kauwe *et al.*, 2014), which we do not consider here; instead these experiments are meant to illustrate the response of biomass and turnover times to an increment in woody-tissue NPP.

In the FACE experiments there was a step increase in CO_2 but we chose a gradual increase in NPP to more closely match the expected increase in atmospheric CO_2. Given, however, that we are mostly concerned with equilibrium rather than transient dynamics, the time frame of the NPP increase is of little importance to results presented here. We used a negative exponential function since the NPP response to increasing CO_2 will likely plateau as other factors (e.g. Nitrogen) become limiting (Zaehle *et al.*, 2014). We model NPP on a given day, NPP_t, as:

$$NPP_t = NPP_0 + ((1 - e^{-\alpha * t}) * \beta * NPP_0) \tag{1}$$

where NPP_0 is NPP prior to simulated eCO2, α determines the rate at which NPP increases, and β determines the final percent increase in NPP, relative to NPP_0. We increased NPP of both understory and canopy cohorts at the same rate ($\alpha = 0.00008$, corresponding to an NPP increase over approximately 100 years), and to the same proportion of initial NPP ($\beta = 0.25$, i.e. a 25% increase). After the onset of the NPP increase, we ran simulations for a further 500 years to reach a new equilibrium.

It is worth noting, that although the increase in NPP here is framed as being a response to eCO_2, in reality, the long-term response of vegetation to eCO_2 remains largely uncertain (Walker *et al.*, 2015; Fisher *et al.*, 2019; Davies-Barnard *et al.*, 2020; Arora *et al.*, 2019). What we are explicitly modelling is an increase in NPP, and, in the context of FATES's prescribed physiology mode, an increase in growth rates, both in terms of height and diameter. Actual vegetation response to eCO_2 will be dependent on a number of variables and may not follow the smooth asymptotic increase that we prescribe here. Increased CO_2 may not result in

increased growth if other factors such as phosphorous become limiting Fleischer *et al.* (2019). Further, any changes to growth rates could also result from rising temperatures, changes in precipitation regimes and ENSO events, and shifts in species compositions (Lewis *et al.*, 2004; Phillips *et al.*, 2009).

While we recognize that choosing a specific number such as 25% is somewhat arbitrary, there have not been FACE experiments conducted in tropical forests, and we expect the idealized results here are qualitatively insensitive to the degree of eNPP; i.e. the ratio of ΔAGB/ΔNPP or $\Delta\tau$/ΔNPP should be roughly consistent across a range of eNPP. We tested this by running background, size- and age-dependent mortality simulations with NPP increases of 10% and 40%, in addition to the 25% increase simulations, which allows us to calculate the ratio of changes in biomass and turnover to changes in woody NPP.

2.2.2 Size- and age-dependent mortality

Size- and age-dependent mortality terms here act in addition to the prescribed background mortality rate and only affect cohorts of large size/age. We represent size-dependent mortality, denoted $mort_s$ as:

$$mort_s = \frac{1}{(1 + e^{-r_s*(DBH-p_s)})} \tag{2}$$

where DBH is diameter at breast height in cm, r_s is the rate that mortality increases with DBH, and p_s is the inflection point of the curve, i.e. the DBH at which the annual mortality rate has increased to 50%. We model age-dependent mortality ($mort_a$) as

$$mort_a = \frac{1}{(1 + e^{-r_a*(age-p_a)})} \tag{3}$$

where age is cohort age in years, and r_a and p_a are the rate at which mortality increases with age and the inflection point, i.e. the age at which annual mortality rate is 50%.

2.2.3 Single PFT simulations

We began with the simplest scenario of a single PFT. We first ran simulations with either background mortality, or background plus either size- or age-dependent mortality. For each mortality scenario (background, size or age) we compared a simulation with constant NPP to one with elevated NPP as described above. We then tested the sensitivity of these scenarios to variation in specification of plant allometries, as well as the sensitivity to the magnitude

of the increase in NPP.

We prescribed canopy and understory growth and background mortality rates such that, at equilibrium, AGB was a reasonable match to the observed values for tropical forests, as presented in (Feeley *et al.*, 2007), table S1.

We parameterised size- and age-dependent mortality functions such that prior to eNPP the size dependency of mortality was approximately equivalent in each of the two scenarios (Fig. 2). In other words, given prescribed growth rates and background mortality, the age-dependent mortality resulted in cohorts dying at the same rate per size as in the size-dependent mortality scenario. Following an increase in growth rates, mortality patterns and carbon dynamics are expected to shift, and the way that they shift will depend on the mechanisms driving mortality. By quantifying these shifts under two end points for size- and age-dependent mortality, we provide a reference to which observations can be matched in order to better understand the mechanisms of mortality.

2.2.4 Carbon turnover times

For all model experiments we calculated the change in AGB, basal area (BA), number of individuals, and carbon turnover time following the onset of eNPP. Carbon turnover time was defined as

$$\tau = \frac{C_{veg}}{NPP} \tag{4}$$

where τ is carbon turnover time at equilibrium, C_{veg} is carbon vegetation (both above ground and below ground), and NPP is net primary productivity.

2.2.5 Sensitivity to allometries

Since we expected that increased growth would allow cohorts to reach larger sizes under age-dependent mortality, we hypothesised that the AGB response to eNPP would be sensitive to allometric equations. We also expected size-dependent mortality results to be sensitive to parameters controlling canopy organisation, given the expected increase in gap formation following eNPP. To test these expectations, we ran ensemble simulations changing the parameterisation of the DBH to height, and the DBH to crown area allometries. We further tested different allometric equations for DBH to height and DBH to AGB.

In both the one PFT and two PFT simulations diameter to height was modelled following

10

O'Brien *et al.* (1995) as

$$h = 10.0^{(log10(DBH)*p_1+p_2)} \tag{5}$$

where h is height in m and DBH is DBH in cm. We used parameters from O'Brien *et al.* (1995); $p_1 = 0.64$ and $p_2 = 0.37$.

Diameter to crown area was modelled as

$$CA = spreadterm * DBH^{d2bl_{p2}} \tag{6}$$

where CA is crown area in m^2, DBH is DBH in cm and $d2bl_{p2}$ is the exponent parameter that alters the scaling of DBH to crown area, set here to 1.3. $spreadterm$ is a site level term that changes through time and alters the spatial spread of tree canopies based on canopy closure.

Diameter to AGB was modelled following Saldarriaga *et al.* (1988) as

$$agb = agbfrac * p_1 * h^{p_2} * d^{p_3} * wd^{p_4} \tag{7}$$

where $agbfrac$ is the carbon fraction of AGB, h is height in m, d is DBH in cm and wd is wood density. We used parameters from Saldarriaga *et al.* (1988); $agbfrac = 0.6$, $p_1 = 0.06896$, $p_2 = 0.572$, $p_3 = 1.94$, $p_4 = 0.931$. In all simulations $wd = 0.7$.

For the allometry sensitivity analysis we first used the allometries above and varied the $p2$ parameter in equation 5 from 0.05 to 0.5, (corresponding to height of 21.4 m to 60.3 m at 100 cm DBH) (Fig. S8) and the $d2bl_{p2}$ parameter in equation 6 from 1.1 to 1.4 (corresponding to a crown area of 91.5 to 364.2 m^2 at 100 cm DBH), (Fig. S9). For each combination of parameters we calculated the change in carbon turnover time and the change in AGB in response to eNPP under both size- and age-dependent mortality.

We then tested different allometric equations. In these simulations we used the same DBH to crown area relationships, but modelled DBH to height following Martínez Cano *et al.* (2019) as

$$h = \frac{(p_1 * DBH^{p_2})}{(p_3 + DBH^{p_2})} \tag{8}$$

where h is height in m and DBH is DBH in cm. We used parameters from Martínez Cano *et al.* (2019); $p_1 = 58$, and $p_3 = 21.8$. We varied p_2 from 0.55 to 2.0 (corresponding to heights

of 21.2 m to 57.7 m at 100 cm DBH) (Fig. S8).

AGB was modelled following Chave *et al.* (2014) as

$$agb = \frac{p_1 * (wd * d^2 * h)^{p_2}}{c2b} \tag{9}$$

where c2b is the carbon to biomass multiplier (here set to 2.0). We used parameters from Chave *et al.* (2014); $p_1 = 0.0673$ and $p_2 = 0.976$.

This allowed us to test both the sensitivity of results to parameter values, along with the sensitivity of results to the choice of allometric equation.

2.2.6   Paired PFT simulations

Elevated growth in response to increasing CO_2 has the potential to change species compositions, and thus functional trait distributions, in tropical forests. Here we tested the effect of a simulated increase in NPP on the co-existence of pairs of PFTs, exploring how the demographic rates of PFTs alters the response to eNPP.

PFT pairs were generated from across observed demographic (growth and survival) parameter space. Canopy mortality and NPP were drawn from a uniform distribution defined in table S1. Pairs of PFTs in which one PFT had both faster growth and lower mortality were discarded on the premise that this would result in competitive exclusion (as illustrated by (Koven *et al.*, 2019)). We generated 100 pairs of PFTs in which PFT 2 had both faster growth and higher mortality than PFT 1, i.e. is relatively more 'early successional'. We impose the condition that PFT 2 also had higher understory background mortality than PFT 1 (0.05 and 0.025 respectively), since mortality rates are presumed to be correlated through ontogeny, and these values were fixed across all pairs. Recruitment, understory NPP, and response to eNPP were equivalent in PFT 1 and 2 and fixed across pairs. Wood density was also equivalent in PFT 1 and PFT 2.

For the two PFT ensembles we ran both size- and age-dependent mortality scenarios with and without NPP increases as described above. We identified pairs of PFTs in the constant NPP scenarios in which one PFT had on average greater than 90% of the total basal area over the last 300 years of the simulation. To retain only co-existing pairs of PFTs, we discarded these ensemble members from both the constant and the matched eNPP ensembles. This left 83 pairs of PFTs with size-dependent mortality and 72 with age-dependent mortality. We used these pairs of PFTs to calculate AGB, BA and τ.

We then used the full set of 100 pairs of PFTs to explore the regions of demographic

12

parameter space that led to dominance by either early or late successional PFTs and also to test how co-existence, AGB and τ changed following eNPP and with alternative representations of plant mortality. We calculated the distance between PFTs in demographic space and also the angle of the slope between them. Large distance between PFTs corresponds to the PFTs being very demographically different (i.e. large differences in canopy NPP and canopy mortality). The angles between PFTs are bounded by 0 and 90, with large angles corresponding to larger differences in NPP relative to differences in mortality. We calculated the change in the percentage plot-level AGB from PFT 2 following eNPP in relation to PFT distance and angle.

3 Results

3.1 Single PFT experiments

We tested three mortality scenarios in the single PFT experiment: constant background mortality, background mortality plus size-dependent mortality, and background mortality plus age-dependent mortality (hereafter referred to as background, size-, or age-dependent). In all three cases simulations with eNPP were compared with constant NPP simulations.

In all mortality scenarios, BA and AGB increased in eNPP simulations relative to the constant NPP simulations (Fig. 3). Differences were greater when mortality was either just background, or age-dependent. Over the last 400 years of the eNPP simulation (i.e. from the point at which NPP had reached its new maximum), the change in AGB was on average 97% that of the increase in NPP (24% increase in biomass, given a 25% increase in NPP) when mortality was age-dependent, and just 54% of the NPP increase (13%, relative to a 25% increase in NPP) when mortality was size-dependent.

With just background mortality, the relative increase in AGB in the eNPP simulations relative to the constant NPP simulations was similar to the age-dependent scenario, 97% of the NPP increase (24%). However, in absolute numbers, the background mortality scenario had much higher BA and AGB in both constant and eNPP simulations, as a result of the greater contribution of large trees to these metrics. For example, mean AGB was 14.5 kgC m^{-2} in constant NPP and 18.0 kgC m^{-2} in eNPP simulations with background mortality. This compares with 10.7 kgC m^{-2} (constant NPP) and 13.3 kgC m^{-2} (eNPP) with age-dependent mortality and 11.5 kgC m^{-2} (constant NPP) and 13.1 kgC m^{-2} (eNPP) with size-dependent mortality.

Regardless of the mortality mechanism, in eNPP simulations, cohorts were growing faster than in constant NPP simulations, and therefore a greater proportion of cohorts reached larger sizes before being killed by background mortality. This resulted in a shift in the size distribution of populations towards larger sizes in all three mortality scenarios under eNPP. A shift in size distributions results in more carbon per unit of crown area as a result of allometric relationships—e.g., as can be seen comparing the exponents in equations 8 and 9 versus equation 6—and hence increased stand-level AGB. The effect was larger when mortality was either just background, or age-dependent (Fig. S1). In the size-dependent mortality simulations 75% of the biomass was in trees $\geq$70 cm DBH with both constant and elevated NPP, because although cohorts grew to larger sizes, they were then killed by the size-dependent mortality term. In contrast, when mortality was age-dependent, 75% of the biomass was in trees $\geq$60 cm DBH with constant NPP, and in trees $\geq$80 cm DBH with eNPP. With just background mortality, trees were much larger than in either size- or age-dependent mortality simulations, and 75% of the biomass shifted from trees $\geq$100 cm DBH to trees $\geq$130 cm DBH in the eNPP compared with constant NPP simulations.

The equilibrium assumption in the definition of τ used in equation 4 means that it can only be evaluated at steady state, once the carbon flux associated with mortality has increased in proportion to NPP. In the background and age-dependent mortality scenarios, this occurs largely due to the increase in size at death, whereas in the size-dependent mortality scenario the rise in mortality-driven carbon loss comes from cohorts reaching the size of elevated death rates sooner. The increase in canopy mortality rates with size-dependent mortality also resulted in a subsequent increase in collateral mortality in the understory, which further decreased τ. Moreover, FATES includes a representation of the perfect plasticity approximation (PPA), whereby all available plot area is filled by cohort canopies. Following canopy growth each time step, a fraction of cohorts are demoted to the understory, so that canopy area remains constant. Increased growth rates result in an increase in this rate of tree demotion to the understory, and since background mortality rates are higher in the understory than in the canopy, there is a subsequent increase in ecosystem level mortality and a further decrease in τ.

Carbon turnover time (τ) therefore decreased under eNPP with all mortality scenarios, although the decrease was largest with size-dependent mortality due to the additional speeding up of tree life cycles (Fig. 3). Over the last 400 years of the simulations, the mean difference in τ between the constant NPP and eNPP simulations was 9.6% with size-dependent mor-

tality. This was a decrease from 27 years to 25 years. With age-dependent mortality, the mean decrease in τ in the constant NPP scenario relative to the eNPP simulation was 2.0%; from 26 to 25 years. The background mortality scenario had a similar response to eNPP as the age-dependent mortality scenario, with a decrease in τ by 2.1%, but again, the absolute numbers were higher, with mean τ equal to 34 years with both constant NPP and eNPP.

3.2 Two PFT experiments

In the two PFT model experiment, we compared only the size- and age-dependent mortality scenarios, and in both cases contrasted simulations with constant NPP to those with eNPP. For each scenario, we ran ensemble simulations in which pairs of PFTs were parameterised with NPP and background mortality rates from across observed demographic space (table S2).

Results from the two PFT model experiments were qualitatively similar to the one PFT experiments. That is, AGB and BA increased following eNPP with both size- and age-dependent mortality, but more so with age-dependent mortality. τ decreased with both mortality scenarios, but more so with size-dependent mortality (Fig. 4). However, there was large variation among ensemble members depending on the position of PFTs in demographic space. In some ensemble members AGB increased relatively more than NPP leading to an increase in τ.

The mean increase in AGB over the last 100 years of simulations in the eNPP relative to the constant NPP simulations ranged from 18.9% to 28.2% across the ensemble, in the age-dependent mortality scenario, with a mean increase of 23.9%. In the size-dependent mortality scenario, the mean increase in AGB in the eNPP relative to the constant NPP simulations ranged from 5.3% to 48.2%, across the ensemble, with a mean increase of 15.0%.

Across the ensemble, the change in τ in the eNPP relative to the constant NPP simulations ranged from -5.2% to 0.3% in the age-dependent mortality scenario, with a mean decrease of -2.4%. In the size-dependent mortality scenario, the mean change in τ in the eNPP relative to the constant NPP simulations ranged from -15.4% to 5.1%, with a mean change of -9.2%. In all two PFT simulations the range of responses to eNPP bracketed the response in the one PFT experiment.

The largest relative increases in AGB were in PFT pairs with low NPP and high background mortality, in both size- and age-dependent mortality scenarios (Fig. 5). These PFT pairs had the lowest initial AGB and saw the largest relative increase in response to eNPP.

The largest decreases in τ were in simulations in which PFT pairs had low canopy background mortality and high canopy NPP, in both size- and age-dependent mortality scenarios (Fig. 5). With size-dependent mortality, low background canopy mortality results in a larger proportion of cohorts reaching the size at which the size-dependent mortality term begins to have an effect, and therefore the speeding up of the life cycle is more apparent in these simulations. High canopy NPP amplifies this effect. With age-dependent mortality, decreases in τ come from increased demotion of cohorts into the understory where background mortality is higher. PFT pairs with high NPP and low background mortality reach larger sizes and therefore demotion rates are higher.

Late successional PFTs (PFT 1) dominated plot-level AGB when the angle between PFTs was low, i.e. when differences in background mortality were large relative to differences in NPP (Fig. 6, top left). This was true for both size- and age-dependent mortality scenarios. PFTs had a more equal proportion of plot AGB when the demographic distance between PFTs was small (Fig. 6, bottom left). As PFTs became more demographically different, one or other tended to dominate.

Five (size-dependent mortality) and nine (age-dependent mortality) ensemble members had a higher proportion of AGB in the late successional PFT in the eNPP simulation compared with constant NPP simulation. In other words, eNPP generally shifted the balance of co-existence in favour of early successional PFTs, even though both PFTs were given the same relative increase in tree-level eNPP. The largest shifts in co-existence in favour of early successional PFTs were in the simulations in which late successional PFTs initially dominated (Fig. 7). This is likely because we increased NPP equally by 25% in both PFTs, which meant a larger absolute increase in NPP for the early successional PFT. There was a negative relationship between the relative increase in the proportion of PFT 2 and the change in plot-level AGB, i.e. those simulations with the greatest plot-level increase in AGB generally had a smaller shift in favour of PFT 2 (Fig. S7). Due to higher background mortality rates, increases in the dominance of PFT 2 shifts the forest towards smaller stature and lower AGB.

Generally, the absolute abundance of both early and late successional PFTs was higher in the eNPP simulations relative to the paired constant NPP simulations. That is, while eNPP shifted the relative abundance of PFTs to favour the early successional PFT, both PFTs still responded positively to the increase in NPP. There were a few exceptions to this, notably there were eleven ensemble members in both size and age dependent mortality

16

scenarios where the absolute AGB of the late successional PFT was actually lower in the eNPP simulation relative to the paired constant NPP simulation.

3.3 Recruitment sensitivity

In the above two PFT experiments, recruitment rates for each PFT were prescribed each time step and were equivalent for both PFTs in each pair, making coexistence more likely. To test the effect of this recruitment scheme on PFT co-existence and the response to eNPP, we repeated the experiment with recruitment based on seed rain from reproductive adults of each PFT, essentially allowing one PFT to competitively exclude the other. Results are shown in Fig. S5. This experiment was with size-dependent mortality only. Far less co-existence occurred in these simulations. In 95 of 100 PFT pairs, one PFT had more than 80% of AGB by the end of the simulation. In the majority of cases (72) it was the early-successional PFT which dominated. Increases in NPP had little effect on co-existence since the early-successional PFT which benefits more from eNPP was already dominant in most ensemble runs.

3.4 Allometry sensitivities

In both size- and age-dependent mortality scenarios, regardless of the allometric equations used (eq. 5, 8, 7 or 9), τ was highest when trees were tall with small crowns (Fig. S11) due to larger vegetation carbon and lower NPP. After the increase in NPP, the largest relative decreases in τ came when mortality was size-dependent and trees were tall with small crowns (Fig. S13). Relative decreases in τ were largest when DBH to height and AGB was modelled using eq. 5 and eq. 7.

The largest increases in AGB in response to eNPP were generally when trees were tall with small crowns, regardless of size- or age-dependent mortality or allometric equations (Fig. S12). Taller trees with smaller crowns allow more cohorts to be in the canopy than the understory, and hence these simulations have both higher τ and AGB. Simulations with a greater proportion of canopy cohorts (small crowns) will have the largest response to eNPP since a greater number of cohorts will be impacted by size and age dependent mortality terms.

3.5   NPP sensitivity

We tested the sensitivity of results to the simulated increase in NPP by running background, size and age-dependent mortality scenarios with elevated NPP of 10% and 40% (Fig. S6). In all cases, ΔAGB/ΔNPP or $\Delta\tau$/ΔNPP were mostly invariant of NPP increase. For example, increases in AGB were 6%, 13% and 20% in the size dependent mortality scenario with increases in NPP of 10%, 25% and 40%, i.e. 50-56% of the increase in NPP. The slopes of regression lines relating the percent change in AGB to the percent change in eNPP were 1.01, 0.48, and 0.92 for the background, size-, and age-dependent mortality cases.

4   Discussion

We used a vegetation demographics model, FATES, to test the effect of size- and age-structured mortality on the carbon dynamics of an idealised tropical forest experiencing a simulated increase in NPP. We found that eNPP increased biomass under both mortality scenarios, but that the increase was only half as large when mortality was a function of tree size. Carbon turnover (τ) decreased in response to eNPP in all mortality scenarios, but the decreases were significantly larger when mortality was a function of size. The response to eNPP was similar in simulations with constant background mortality scenario (no size or age dependent mortality) to those with age-dependent mortality. However, with neither size- nor age-dependent mortality, cohorts reached much larger sizes and both absolute biomass and τ were higher (Fig. 3).

These results were qualitatively the same in two PFT ensembles in which growth and survival rates of PFTs were sampled from across demographic space. However, the magnitude of the eNPP effect depended on demographic rates and the similarity of PFTs. Further, we find that allometric equations have a large influence on the simulated eNPP response, altering both the increase in AGB and the decrease in τ.

4.1   Increases in aboveground biomass

Elevated NPP led to an increase in forest biomass with both size- and age-dependent mortality, and in simulations with constant background mortality (Fig. 3). While the AGB increases with just background mortality and with age-dependent mortality matched expectations, the increase in biomass under eCO2 with size-dependent mortality is less intuitive, but results from a shift in the size distribution towards larger sizes. As growth rates increase,

18

cohorts reach larger sizes before they are killed from the background mortality rate. Therefore, although the size-dependent mortality term does not change, following an increase in growth rates, a larger proportion of cohorts make it to the size at which the size-dependent mortality term takes effect. In FATES, background mortality accounts for sources of mortality that are not explicitly modelled. For all simulations here (which were run in prescribed physiology mode and thus not subject to physiologically driven carbon starvation, hydraulic failure or fire induced mortality) , it is the predominant source of mortality for both canopy and understory cohorts. If the risk of mortality from these phsiological mechanisms and disturbance events remains constant over much of the life cycle, then increases in productivity may result in increases in AGB, with the magnitude depending on whether mortality risk increases with tree size or age.

Observations of natural forests have so far shown mixed evidence of a CO_2 fertilisation effect. Clark *et al.* (2013) found no increase in NPP in a Costa Rican forest from 1997-2009 and concluded that any CO_2 fertilisation effect was being offset by climate related stress. Monitoring of forest plots across the Amazon, however, have found mortality to be positively correlated with productivity, with increases in mortality lagging behind increases in productivity, supporting the hypothesis of a CO_2 induced increase in both biomass and mortality (Brienen *et al.*, 2015).

4.2 Decreases in carbon turnover time

In our experiments, background, size, and age-dependent mortality led to a decrease in τ (Fig. 3). This is in line with predictions for size-dependent mortality scenarios due to a speeding up of the life cycle (Büntgen *et al.*, 2019). In addition, regardless of the mechanism of mortality, τ decreased due to an increase in the proportion of cohorts in the understory. In FATES, the perfect plasticity approximation algorithm assumes that all available plot area is filled by cohort crowns. As the population shifts towards larger sizes, there are fewer trees in the canopy, since each of their crown areas are larger. Each time step, as crowns expand, a number of trees in each canopy cohort are demoted to the understory to keep plot level canopy area constant. Under eNPP, this demotion occurs more rapidly, and thus there is an ecosystem level increase in mortality due to the higher background mortality of understory cohorts, and a subsequent decrease in τ. Demotion of cohorts to the understory represents overtopping, whereby individuals in gaps become shaded by faster growing neighbours. This phenomenon is widespread in closed canopy forests and periods of

19

time spent in gaps and then shade can explain growth trajectories of forest trees (Brienen & Zuidema, 2006; Metcalf *et al.*, 2009). Our result - where increased growth leads to an increase in overtopping and consequently higher understory mortality - matches theory on accelerated successional dynamics, e.g. Harper (1977); Clark (1990). In particular, results are analogous to the enhanced asymmetric competition hypothesis described by Stephenson *et al.* (2011) whereby increased resources enhance the growth of the largest individuals, which then more quickly suppress smaller trees leading to elevated mortality of suppressed trees. Our results suggest that any increases in growth rates are likely to be accompanied by a decrease in τ, although the mechanisms driving mortality will determine the extent of the decrease, with potentially important implications for terrestrial carbon storage dynamics of ESMs.

At the same time, there is a compensating effect, whereby the amount of biomass able to be stored in trees within a given canopy strata is increased due the allometrically-determined ratio of AGB to crown area for a given tree, which increases with larger tree sizes. In the background and age-dependent mortality cases, this effect is almost sufficient to cancel the reduction in turnover times resulting from increased light competition and mortality, whereas in the size-dependent mortality case the extra increment of increased mortality resulting from senescence is able reduce by approximately half the expected increase in AGB.

4.3   Implications for carbon dynamics

It has been argued previously that reductions in τ following eCO$_2$ could offset any benefit from increased growth in terms of mitigating anthropogenic carbon emissions, as the increase in carbon uptake is counteracted by the increase in mortality and decomposition rates (Körner, 2017; Büntgen *et al.*, 2019). The extent to which trees grow to larger sizes and/or move through their life cycles more rapidly could therefore have a large impact on the magnitude of increases in carbon stocks and the decreases in carbon turnover.

These results suggest that if eCO$_2$ causes increases in NPP in line with what we simulate here (a 25% increase), then increases in AGB will result, albeit at a reduced level as compared to the change in eNPP, despite simultaneous decreases in tree life spans. This is in contrast to Bugmann & Bigler (2011) who used a factorial design of changing growth-longevity relationships under different growth simulation effects to test the impact of these parameterisations on forest biomass and carbon turnover time using the gap model ForClim. Bugmann & Bigler (2011) found that increases in biomass were small (even in growth simulation only experiments) and were mostly offset by reductions in longevity. These differences

could be due to a number of structural assumptions within ForClim and FATES, as well as the model parameterisations. In particular, increases in biomass in our size-dependent mortality scenario came from trees reaching larger sizes before being killed by background mortality. Bugmann & Bigler (2011) assume that reductions in longevity are manifested as an increase in the background mortality term and thus do not see the same effect of a shift in the size at death, and a consequent increase in AGB.

Although there is evidence for a trade-off between growth and survival at the individual level (Bigler & Veblen, 2009; Di Filippo *et al.*, 2012) it is not clear if increased growth from eCO_2 will directly result in reductions in longevity. Trade-offs result from allocation of limited resources between growth, and defence and maintenance traits that increase survival. All else remaining equal, eCO_2 is essentially increasing the resources available to individuals, and thus might increase growth rates without compromising survival. However, tree ring analysis of individuals that were juveniles both pre and post industrial revolution found a negative relationship between juvenile growth rates and longevity (Büntgen *et al.*, 2019).

Further, observations of biomass trends in the Amazon suggest CO_2 driven increases in productivity, followed by lagged increases in mortality. More recent levelling off of growth rates in the last few decades, combined with continuously increasing mortality is leading to a decrease in carbon residence time and a decrease in the rate of net carbon accumulation (Brienen *et al.*, 2015; Hubau *et al.*, 2020). Continued monitoring of forest tree demographic rates are needed over larger spatial and temporal scales in order to understood whether elevated growth under eCO_2 will speed up tree life cycles or allow trees to reach larger sizes. Changes in plant mortality may, of course, result from changes in climate conditions as well as from eCO_2 driven dynamics, and so simultaneous efforts to understand, model and observe these will also be necessary to predict the overall changes in forest dynamics in the real world (McDowell *et al.*, 2018).

4.4   Uncertainties in forest response to eCO_2

In addition, the growth response of forests to eCO_2 remains uncertain (Walker *et al.*, 2015). We simulated forest response to eCO_2 as a gradual increase in NPP that asymptotes at 25% above the starting value after approximately 100 years; the magnitude of the increase intended to match the observed increase in NPP at the Duke and ORNL FACE experiments. However, FACE experiments have shown that the response of forest stands to eCO_2, in the short term at least, is largely determined by nutrient cycling (Zaehle *et al.*, 2014). High

21

plant N uptake and N use efficiency (NUE) at Duke allowed a sustained NPP response to eCO$_2$, while at ORNL a decrease in NUE from increased allocation to N-rich fine roots led to a decrease in the NPP response. How these processes are represented in vegetation models can lead to a divergence of model predictions of forest response to eCO$_2$ (Zaehle *et al.*, 2014; Walker *et al.*, 2015; Fisher *et al.*, 2019; Davies-Barnard *et al.*, 2020).

Extrapolations from CO$_2$ enrichment experiments to the global scale find strong nutrient constraints on the vegetation response to CO$_2$, but predict a 12.5% increase in tropical forest AGB by 2100 (Terrer *et al.*, 2019). Likewise, ensemble model runs that explicitly incorporate phosphorus (P) cycling, suggest that P limitation across the Amazon could strongly reduce the effect of eCO$_2$ on carbon sequestration (Fleischer *et al.*, 2019). It is, therefore, worth noting that the 25% increase in NPP that we simulate here may be at the high end of what is likely to be observed over the next century, especially in regions where other resources are limiting. Our sensitivity analysis, however, revealed a mostly invariant response of AGB and τ to the simulated increase in productivity; that is ratio of $\Delta AGB / \Delta NPP$ varied little for NPP values of 10, 25 and 40%.

Since we are interested in the effects of increased growth rates, and the interaction with mortality, on carbon storage, we can overlook the effects of root and leaf turnover. However, it is worth noting that carbon turnover time also depends on turnover of biomass from leaves and fine roots (Norby *et al.*, 2002; Kauwe *et al.*, 2014), and a 25% in NPP may not result in the increase in growth and biomass that we report here. Thus these experiments serve as a simple test to understand only changes to the woody biomass component of ecosystems, assuming no changes to allometry or allocation as a result of the eCO$_2$ treatment.

4.5 Changes to co-existence

In our two PFT simulations, coexistence depended on the degree of demographic similarity between PFTs, (following (Koven *et al.*, 2019)) (Fig. 7). Simulations varied from competitive exclusion by late successional PFTs, through equal abundance of PFTs, to competitive exclusion by early successional PFTs (Fig. 6). In all these cases, increasing NPP of both PFTs by 25% did little to change the relative proportion of each PFT in terms of AGB. Any changes in the proportion of PFTs tended to be in favour of the early successional PFT. This is likely because we increased NPP of both PFTs by 25%, and since the early succcessional PFT had a higher NPP to begin with, it had a larger absolute increase in NPP.

In our 2-PFT simulations both PFTs had either size–dependent or age-dependent mor-

tality. In reality, it is possible that competing species may differ in their mortality patterns; some species response to eCO_2 will be more similar to the age-dependent mortality scenario, while other species might show a more size-dependent mortality response. Further, growth increases might be larger in some species than others. For instance, species with faster growth rates may respond more to eCO_2 than slow growing species (Laurance *et al.*, 2004). At one extreme of this continuum are lianas, which have strong growth responses to CO_2 concentrations (Granados & Körner, 2002) and have been found to be increasing in Amazonian forests, possibly as a result of CO_2 fertilisation (Phillips *et al.*, 2002). However, in a study of ten large tropical plots Chave *et al.* (2008) found that the absolute biomass of slow growing species was increasing across plots, suggesting that fast growing species are not replacing slow growing species. Finally, PFTs in our experiments differed only in rates of canopy mortality and NPP, and thus we missed other potentially important elements of natural variation that could influence the CO_2 response or estimates of biomass. For example, we kept wood density the same across PFTs but there is evidence that faster growing species tend to have lower wood density e.g. (Chave *et al.*, 2009). Had we made wood density lower in the early succesional PFT, we might have seen more of an effect of eNPP on plot level AGB, due to shifts in the proportions of the two PFTs. These results, however, show that even if eCO2 affects early and late successional individuals equally, it may promote early-successional species populations more than late successional one. In future work, we will incorporate these senescence mortality terms into the full-complexity FATES model, to explore how more physiologically mechanistic predictions of changes to plant growth and mortality rates across functionally varying PFTs, under elevated CO_2 and climate change result in changes to the AGB and τ terms we focus on here.

For the majority of species it is not clear what determines maximum size. In the tallest species, hydraulic constraints limit individual tree height (Koch *et al.*, 2004; Niklas & Spatz, 2004; Domec *et al.*, 2008), which will prevent these species from reaching larger sizes despite increased growth rates. For those species at least, we expect to see a size-dependent mortality type response to eCO_2, i.e. a small increase in ABG due to the lower effects of background mortality, but a larger decrease in carbon turnover time. It is likely that the maximum size of most species is related to shifts in allocation strategies; i.e, at large sizes resources are allocated to reproduction rather than growth and maintenance, thus increasing the risk of mortality (Wheelwright & Logan, 2004; Genet *et al.*, 2009). This would explain why, despite the trend of increasing growth with size at the population level (Stephenson *et al.*, 2014),

individual trees show a decrease in growth immediately preceding death e.g. (Arellano *et al.*, 2019). Monocarpic species might represent the extreme of this phenomenon; as following reproduction the whole tree dies e.g. (Foster, 1977; Read *et al.*, 2006). If maximum size is related to trees balancing investment of limited resources between reproduction, growth and maintenance, then with all else remaining equal, increased CO_2 may allow trees to reach larger sizes, reproduce younger (Ladeau & Clark, 2006), or both. As such, allocation strategies (to fast or slow turnover carbon pools) at large size will likely have important implications for large scale carbon storage (Pugh *et al.*, 2020).

4.6   Conclusions

Forest responses to rising CO_2 represent a major source of uncertainty in projections of future climate. In particular, a reduction in carbon turnover time due to trees moving through their life cycles more quickly could offset any potential for forests to mitigate anthropogenic carbon emissions. Here we quantify the effects of both size- and age-dependent mortality on carbon dynamics using a reduced-complexity version of the vegetation demographic model FATES and compare them with simulations using only default background mortality. We find that simulated increases in NPP (from an assumed increase in CO_2) combined with either size- and age-dependent mortality will lead to shifts in the size distributions of populations and increases in forest biomass, relative to simulations with constant NPP. Reductions in carbon turnover time with size-dependent mortality were smaller than the increases in forest biomass following a simulated increase in productivity. While the relative response to increased productivity was similar in the background mortality simulations to the age-dependent simulations - large increases in AGB and small increases in τ - the absolute values of AGB and τ were much higher with background mortality, suggesting that explicit representations of the scaling of mortality mechanisms with size or age will be essential for improved representation of forest response to eCO_2 in projections of future climate.

5   Acknowledgements

6 Author Contributions

CDK, RGK, RAF and JFN contributed to the development of the FATES model. JFN and CDK designed model experiments, JFN performed model experiments and analysed model output with input from CDK, RGK and RAF. JFN wrote the manuscript with input from all authors.

7 Competing Interests

The authors declare no competing interests.

8 Final Version

This is the pre-peer reviewed version of the following article: Needham, J.F., Chambers, J., Fisher, R., Knox, R. and Koven, C.D. (2020), Forest responses to simulated elevated CO2 under alternate hypotheses of size- and age-dependent mortality. Glob Change Biol. Accepted Author Manuscript. doi:10.1111/gcb.15254

which has been published in final form at [https://doi.org/10.1111/gcb.15254]. This article may be used for non-commercial purposes in accordance with Wiley Terms and Conditions for Use of Self-Archived Versions.

References

Ainsworth, E.A. & Long, S.P. (2005). What have we learned from 15 years of free-air CO2 enrichment (FACE)? A meta-analytic review of the responses of photosynthesis, canopy properties and plant production to rising CO2. *New Phytologist*, 165, 351–372.

Arellano, G., Medina, N.G., Tan, S., Mohamad, M. & Davies, S.J. (2019). Crown damage and the mortality of tropical trees. *New Phytologist*, 221, 169–179.

Arora, V.K. & Boer, G.J. (2006). Simulating competition and coexistence between plant functional types in a dynamic vegetation model. *Earth Interactions*, 10, 1–30.

Arora, V.K., Katavouta, A., Williams, R.G., Jones, C.D., Brovkin, V., Friedlingstein, P., Schwinger, J., Bopp, L., Boucher, O., Cadule, P. *et al.* (2019). Carbon-concentration and carbon-climate feedbacks in cmip6 models, and their comparison to cmip5 models. *Biogeosciences Discussions*, pp. 1–124.

Bennett, A.C., McDowell, N.G., Allen, C.D. & Anderson-Teixeira, K.J. (2015). Larger trees suffer most during drought in forests worldwide. *Nature Plants*, 1, 15139 EP –.

Bigler, C. & Veblen, T.T. (2009). Increased early growth rates decrease longevities of conifers in subalpine forests. *Oikos*, 118, 1130–1138.

Brienen, R. & Zuidema, P. (2006). Lifetime growth patterns and ages of Bolivian rain forest trees obtained by tree ring analysis. *Journal of Ecology*, 94, 481–493.

Brienen, R.J.W., Phillips, O.L., Feldpausch, T.R., Gloor, E., Baker, T.R., Lloyd, J., Lopez-Gonzalez, G., Monteagudo-Mendoza, A., Malhi, Y., Lewis, S.L., Vásquez Martinez, R., Alexiades, M., Álvarez Dávila, E., Alvarez-Loayza, P., Andrade, A., Aragão, L.E.O.C., Araujo-Murakami, A., Arets, E.J.M.M., Arroyo, L., Aymard C., G.A., Bánki, O.S., Baraloto, C., Barroso, J., Bonal, D., Boot, R.G.A., Camargo, J.L.C., Castilho, C.V., Chama, V., Chao, K.J., Chave, J., Comiskey, J.A., Cornejo Valverde, F., da Costa, L., de Oliveira, E.A., Di Fiore, A., Erwin, T.L., Fauset, S., Forsthofer, M., Galbraith, D.R., Grahame, E.S., Groot, N., Hérault, B., Higuchi, N., Honorio Coronado, E.N., Keeling, H., Killeen, T.J., Laurance, W.F., Laurance, S., Licona, J., Magnussen, W.E., Marimon, B.S., Marimon-Junior, B.H., Mendoza, C., Neill, D.A., Nogueira, E.M., Núñez, P., Pallqui Camacho, N.C., Parada, A., Pardo-Molina, G., Peacock, J., Peña-Claros, M., Pickavance, G.C., Pitman, N.C.A., Poorter, L., Prieto, A., Quesada, C.A., Ramírez, F., Ramírez-Angulo, H., Restrepo, Z., Roopsind, A., Rudas, A., Salomão, R.P., Schwarz, M., Silva, N., Silva-Espejo, J.E., Silveira, M., Stropp, J., Talbot, J., ter Steege, H., Teran-Aguilar, J., Terborgh, J., Thomas-Caesar, R., Toledo, M., Torello-Raventos, M., Umetsu, R.K., van der Heijden, G.M.F., van der Hout, P., Guimarães Vieira, I.C., Vieira, S.A., Vilanova, E., Vos, V.A. & Zagt, R.J. (2015). Long-term decline of the amazon carbon sink. *Nature*, 519, 344 EP –.

Bugmann, H. & Bigler, C. (2011). Will the co2 fertilization effect in forests be offset by reduced tree longevity? *Oecologia*, 165, 533–544.

Bugmann, H., Seidl, R., Hartig, F., Bohn, F., Brůna, J., Cailleret, M., François, L., Heinke, J., Henrot, A.J., Hickler, T., H ulsmann, L., Huth, A., Jacquemin, I., Kollas, C., Lasch-

Born, P., Lexer, M.J., Merganič, J., Merganičová, K., Mette, T., Miranda, B.R., Nadal-Sala, D., Rammer, W., Rammig, A., Reineking, B., Roedig, E., Sabaté, S., Steinkamp, J., Suckow, F., Vacchiano, G., Wild, J., Xu, C. & Reyer, C.P.O. (2019). Tree mortality submodels drive simulated long-term forest dynamics: assessing 15 models from the stand to global scale. *Ecosphere*, 10, e02616.

Büntgen, U., Krusic, P.J., Piermattei, A., Coomes, D.A., Esper, J., Myglan, V.S., Kirdyanov, A.V., Camarero, J.J., Crivellaro, A. & Körner, C. (2019). Limited capacity of tree growth to mitigate the global greenhouse effect under predicted warming. *Nature Communications*, 10, 2171.

Canham, C.D., Finzi, A.C., Pacala, S.W. & Burbank, D.H. (1994). Causes and consequences of resource heterogeneity in forests: interspecific variation in light transmission by canopy trees. *Canadian Journal of Forest Research*, 24, 337–349.

Chave, J., Condit, R., Muller-Landau, H.C., Thomas, S.C., Ashton, P.S., Bunyavejchewin, S., Co, L.L., Dattaraja, H.S., Davies, S.J., Esufali, S., Ewango, C.E.N., Feeley, K.J., Foster, R.B., Gunatilleke, N., Gunatilleke, S., Hall, P., Hart, T.B., Hernández, C., Hubbell, S.P., Itoh, A., Kiratiprayoon, S., LaFrankie, J.V., Loo de Lao, S., Makana, J., Noor, M.N.S., Kassim, A.R., Samper, C., Sukumar, R., Suresh, H.S., Tan, S., Thompson, J., Tongco, M.D.C., Valencia, R., Vallejo, M., Villa, G., Yamakura, T., Zimmerman, J.K. & Losos, E.C. (2008). Assessing evidence for a pervasive alteration in tropical tree communities. *PLOS Biology*, 6, 1–8.

Chave, J., Coomes, D., Jansen, S., Lewis, S.L., Swenson, N.G. & Zanne, A.E. (2009). Towards a worldwide wood economics spectrum. *Ecology Letters*, 12, 351–366.

Chave, J., Réjou-Méchain, M., Búrquez, A., Chidumayo, E., Colgan, M.S., Delitti, W.B., Duque, A., Eid, T., Fearnside, P.M., Goodman, R.C., Henry, M., Martínez-Yrízar, A., Mugasha, W.A., Muller-Landau, H.C., Mencuccini, M., Nelson, B.W., Ngomanda, A., Nogueira, E.M., Ortiz-Malavassi, E., Pélissier, R., Ploton, P., Ryan, C.M., Saldarriaga, J.G. & Vieilledent, G. (2014). Improved allometric models to estimate the aboveground biomass of tropical trees. *Global Change Biology*, 20, 3177–3190.

Clark, D.A., Clark, D.B. & Oberbauer, S.F. (2013). Field-quantified responses of tropical rainforest aboveground productivity to increasing co2 and climatic stress, 1997–2009. *Journal of Geophysical Research: Biogeosciences*, 118, 783–794.

Clark, J.S. (1990). Integration of ecological levels: Individual plant growth, population mortality and ecosystem processes. *Journal of Ecology*, 78, 275–299.

da Costa, A.C.L., Galbraith, D., Almeida, S., Portela, B.T.T., da Costa, M., Junior, J.d.A.S., Braga, A.P., de Gonçalves, P.H., de Oliveira, A.A., Fisher, R. *et al.* (2010). Effect of 7 yr of experimental drought on vegetation dynamics and biomass storage of an eastern amazonian rainforest. *New Phytologist*, 187, 579–591.

Davies-Barnard, T., Meyerholt, J., Zaehle, S., Friedlingstein, P., Brovkin, V., Fan, Y., Fisher, R.A., Jones, C.D., Lee, H., Peano, D. *et al.* (2020). Nitrogen cycling in cmip6 land surface models: Progress and limitations. *Biogeosciences Discussions*.

Di Filippo, A., Biondi, F., Maugeri, M., Schirone, B. & Piovesan, G. (2012). Bioclimate and growth history affect beech lifespan in the italian alps and apennines. *Global Change Biology*, 18, 960–972.

Domec, J.C., Lachenbruch, B., Meinzer, F.C., Woodruff, D.R., Warren, J.M. & McCulloh, K.A. (2008). Maximum height in a conifer is associated with conflicting requirements for xylem design. *Proceedings of the National Academy of Sciences*, 105, 12069–12074.

E3SM Project, D. (2018). Energy exascale earth system model. [Computer Software] `https://doi.org/10.11578/E3SM/dc.20180418.36`.

Farrior, C.E., Bohlman, S.A., Hubbell, S. & Pacala, S.W. (2016). Dominance of the suppressed: Power-law size structure in tropical forests. *Science*, 351, 155–157.

Feeley, K.J., Davies, S.J., Ashton, P.S., Bunyavejchewin, S., Nur Supardi, M., Kassim, A.R., Tan, S. & Chave, J. (2007). The role of gap phase processes in the biomass dynamics of tropical forests. *Proceedings of the Royal Society B: Biological Sciences*, 274, 2857–2864.

Fisher, R., McDowell, N., Purves, D., Moorcroft, P., Sitch, S., Cox, P., Huntingford, C., Meir, P. & Woodward, F.I. (2010). Assessing uncertainties in a second-generation dynamic vegetation model caused by ecological scale limitations. *New Phytologist*, 187, 666–681.

Fisher, R.A. & Koven, C.D. (2020). Perspectives on the future of land surface models and the challenges of representing complex terrestrial systems. *Journal of Advances in Modeling Earth Systems*.

Fisher, R.A., Koven, C.D., Anderegg, W.R.L., Christoffersen, B.O., Dietze, M.C., Farrior, C.E., Holm, J.A., Hurtt, G.C., Knox, R.G., Lawrence, P.J., Lichstein, J.W., Longo, M.,

Matheny, A.M., Medvigy, D., Muller-Landau, H.C., Powell, T.L., Serbin, S.P., Sato, H., Shuman, J.K., Smith, B., Trugman, A.T., Viskari, T., Verbeeck, H., Weng, E., Xu, C., Xu, X., Zhang, T. & Moorcroft, P.R. (2018). Vegetation demographics in earth system models: A review of progress and priorities. *Global Change Biology*, 24, 35–54.

Fisher, R.A., Muszala, S., Verteinstein, M., Lawrence, P., Xu, C., McDowell, N.G., Knox, R.G., Koven, C., Holm, J., Rogers, B.M., Spessa, A., Lawrence, D. & Bonan, G. (2015). Taking off the training wheels: the properties of a dynamic vegetation model without climate envelopes, clm4.5(ed). *Geoscientific Model Development*, 8, 3593–3619.

Fisher, R.A., Wieder, W.R., Sanderson, B.M., Koven, C.D., Oleson, K.W., Xu, C., Fisher, J.B., Shi, M., Walker, A.P. & Lawrence, D.M. (2019). Parametric controls on vegetation responses to biogeochemical forcing in the clm5. *Journal of Advances in Modeling Earth Systems*, 11, 2879–2895.

Fleischer, K., Rammig, A., De Kauwe, M.G., Walker, A.P., Domingues, T.F., Fuchslueger, L., Garcia, S., Goll, D.S., Grandis, A., Jiang, M., Haverd, V., Hofhansl, F., Holm, J.A., Kruijt, B., Leung, F., Medlyn, B.E., Mercado, L.M., Norby, R.J., Pak, B., von Randow, C., Quesada, C.A., Schaap, K.J., Valverde-Barrantes, O.J., Wang, Y.P., Yang, X., Zaehle, S., Zhu, Q. & Lapola, D.M. (2019). Amazon forest response to co2 fertilization dependent on plant phosphorus acquisition. *Nature Geoscience*, 12, 736–741.

Fonseca, M.G., Vidal, E. & Maës dos Santos, F.A. (2009). Intraspecific variation in the fruiting of an amazonian timber tree: Implications for management. *Biotropica*, 41, 179–185.

Foster, R.B. (1977). Tachigalia versicolor is a suicidal neotropical tree. *Nature*, 268, 624–626.

Friend, A.D., Lucht, W., Rademacher, T.T., Keribin, R., Betts, R., Cadule, P., Ciais, P., Clark, D.B., Dankers, R., Falloon, P.D., Ito, A., Kahana, R., Kleidon, A., Lomas, M.R., Nishina, K., Ostberg, S., Pavlick, R., Peylin, P., Schaphoff, S., Vuichard, N., Warszawski, L., Wiltshire, A. & Woodward, F.I. (2014). Carbon residence time dominates uncertainty in terrestrial vegetation responses to future climate and atmospheric CO_2. *Proceedings of the National Academy of Sciences*, 111, 3280–3285.

Genet, H., Bréda, N. & Dufrêne, E. (2009). Age-related variation in carbon allocation at tree and stand scales in beech (Fagus sylvatica L.) and sessile oak (Quercus petraea (Matt.) Liebl.) using a chronosequence approach. *Tree Physiology*, 30, 177–192.

Gonzalez-Akre, E., Meakem, V., Eng, C.Y., Tepley, A.J., Bourg, N.A., McShea, W., Davies, S.J. & Anderson-Teixeira, K. (2016). Patterns of tree mortality in a temperate deciduous forest derived from a large forest dynamics plot. *Ecosphere*, 7, e01595.

Granados, J. & K orner, C. (2002). In deep shade, elevated co2 increases the vigor of tropical climbing plants. *Global Change Biology*, 8, 1109–1117.

Harper, J.L. (1977). *Population biology of plants*. Academic Press, New York, USA.

Heineman, K.D., Russo, S.E., Baillie, I.C., Mamit, J.D., Chai, P.P.K., Chai, L., Hindley, E.W., Lau, B.T., Tan, S. & Ashton, P.S. (2015). Influence of tree size, taxonomy, and edaphic conditions on heart rot in mixed-dipterocarp Bornean rainforests: implications for aboveground biomass estimates. *Biogeosciences Discussions*, 12, 6821–6861.

Hendrey, G.R., Ellsworth, D.S., Lewin, K.F. & Nagy, J. (1999). A free-air enrichment system for exposing tall forest vegetation to elevated atmospheric co2. *Global Change Biology*, 5, 293–309.

Herrick, J.D. & Thomas, R.B. (1999). Effects of CO2 enrichment on the photosynthetic light response of sun and shade leaves of canopy sweetgum trees (Liquidambar styraciflua) in a forest ecosystem. *Tree Physiology*, 19, 779–786.

Hubau, W., Lewis, S.L., Phillips, O.L., Affum-Baffoe, K., Beeckman, H., Cuní-Sanchez, A., Daniels, A.K., Ewango, C.E.N., Fauset, S., Mukinzi, J.M., Sheil, D., Sonké, B., Sullivan, M.J.P., Sunderland, T.C.H., Taedoumg, H., Thomas, S.C., White, L.J.T., Abernethy, K.A., Adu-Bredu, S., Amani, C.A., Baker, T.R., Banin, L.F., Baya, F., Begne, S.K., Bennett, A.C., Benedet, F., Bitariho, R., Bocko, Y.E., Boeckx, P., Boundja, P., Brienen, R.J.W., Brncic, T., Chezeaux, E., Chuyong, G.B., Clark, C.J., Collins, M., Comiskey, J.A., Coomes, D.A., Dargie, G.C., de Haulleville, T., Kamdem, M.N.D., Doucet, J.L., Esquivel-Muelbert, A., Feldpausch, T.R., Fofanah, A., Foli, E.G., Gilpin, M., Gloor, E., Gonmadje, C., Gourlet-Fleury, S., Hall, J.S., Hamilton, A.C., Harris, D.J., Hart, T.B., Hockemba, M.B.N., Hladik, A., Ifo, S.A., Jeffery, K.J., Jucker, T., Yakusu, E.K., Kearsley, E., Kenfack, D., Koch, A., Leal, M.E., Levesley, A., Lindsell, J.A., Lisingo, J., Lopez-Gonzalez, G., Lovett, J.C., Makana, J.R., Malhi, Y., Marshall, A.R., Martin, J., Martin, E.H., Mbayu, F.M., Medjibe, V.P., Mihindou, V., Mitchard, E.T.A., Moore, S., Munishi, P.K.T., Bengone, N.N., Ojo, L., Ondo, F.E., Peh, K.S.H., Pickavance, G.C., Poulsen, A.D., Poulsen, J.R., Qie, L., Reitsma, J., Rovero, F., Swaine, M.D., Talbot, J., Taplin, J.,

Taylor, D.M., Thomas, D.W., Toirambe, B., Mukendi, J.T., Tuagben, D., Umunay, P.M., van der Heijden, G.M.F., Verbeeck, H., Vleminckx, J., Willcock, S., Wöll, H., Woods, J.T. & Zemagho, L. (2020). Asynchronous carbon sink saturation in african and amazonian tropical forests. *Nature*, 579, 80–87.

Kauwe, M.G.D., Medlyn, B.E., Zaehle, S., Walker, A.P., Dietze, M.C., Wang, Y., Luo, Y., Jain, A.K., El-Masri, B., Hickler, T., Wårlind, D., Weng, E., Parton, W.J., Thornton, P.E., Wang, S., Prentice, I.C., Asao, S., Smith, B., McCarthy, H.R., Iversen, C.M., Hanson, P.J., Warren, J.M., Oren, R. & Norby, R.J. (2014). Where does the carbon go? a model–data intercomparison of vegetation carbon allocation and turnover processes at two temperate forest free-air co2 enrichment sites. *New Phytologist*, 203, 883–899.

Klimešová, J., Nobis, M.P. & Herben, T. (2015). Senescence, ageing and death of the whole plant: morphological prerequisites and constraints of plant immortality. *New Phytologist*, 206, 14–18.

Koch, G.W., Sillett, S.C., Jennings, G.M. & Davis, S.D. (2004). The limits to tree height. *Nature*, 428, 851–854.

Körner, C. (2017). A matter of tree longevity. *Science*, 355, 130–131.

Koven, C., Riley, W., Knox, R., Chambers, J. & Negrón-Juárez, R. (2015a). Observed allocations of productivity and biomass, and turnover times in tropical forests are not accurately represented in cmip5 earth system models. *Environmental Research Letters*, 10.

Koven, C.D., Chambers, J.Q., Georgiou, K., Knox, R., Negron-Juarez, R., Riley, W.J., Arora, V.K., Brovkin, V., Friedlingstein, P. & Jones, C.D. (2015b). Controls on terrestrial carbon feedbacks by productivity versus turnover in the CMIP5 Earth System Models. *Biogeosciences*, 12, 5211–5228.

Koven, C.D., Knox, R.G., Fisher, R.A., Chambers, J., Christoffersen, B.O., Davies, S.J., Detto, M., Dietze, M.C., Faybishenko, B., Holm, J., Huang, M., Kovenock, M., Kueppers, L.M., Lemieux, G., Massoud, E., McDowell, N.G., Muller-Landau, H.C., Needham, J.F., Norby, R.J., Powell, T., Rogers, A., Serbin, S.P., Shuman, J.K., Swann, A.L.S., Varadharajan, C., Walker, A.P., Wright, S.J. & Xu, C. (2019). Benchmarking and parameter sensitivity of physiological and vegetation dynamics using the functionally assembled

terrestrial ecosystem simulator (fates) at barro colorado island, panama. *Biogeosciences Discussions*, 2019, 1–46.

Ladeau, S.L. & Clark, J.S. (2006). Elevated co2 and tree fecundity: the role of tree size, interannual variability, and population heterogeneity. *Global Change Biology*, 12, 822–833.

Lagergren, F., J onsson, A.M., Blennow, K. & Smith, B. (2012). Implementing storm damage in a dynamic vegetation model for regional applications in sweden. *Ecological Modelling*, 247, 71 – 82.

Laurance, W.F., Oliveira, A.A., Laurance, S.G., Condit, R., Nascimento, H.E.M., Sanchez-Thorin, A.C., Lovejoy, T.E., Andrade, A., D'Angelo, S., Ribeiro, J. & Dick, C.W. (2004). Pervasive alteration of tree communities in undisturbed amazonian forests. *Nature*, 428, 171–175.

Lawrence, D.M., Fisher, R.A., Koven, C.D., Oleson, K.W., Swenson, S.C., Bonan, G., Collier, N., Ghimire, B., van Kampenhout, L., Kennedy, D., Kluzek, E., Lawrence, P.J., Li, F., Li, H., Lombardozzi, D., Riley, W.J., Sacks, W.J., Shi, M., Vertenstein, M., Wieder, W.R., Xu, C., Ali, A.A., Badger, A.M., Bisht, G., van den Broeke, M., Brunke, M.A., Burns, S.P., Buzan, J., Clark, M., Craig, A., Dahlin, K., Drewniak, B., Fisher, J.B., Flanner, M., Fox, A.M., Gentine, P., Hoffman, F., Keppel-Aleks, G., Knox, R., Kumar, S., Lenaerts, J., Leung, L.R., Lipscomb, W.H., Lu, Y., Pandey, A., Pelletier, J.D., Perket, J., Randerson, J.T., Ricciuto, D.M., Sanderson, B.M., Slater, A., Subin, Z.M., Tang, J., Thomas, R.Q., Val Martin, M. & Zeng, X. (2019). The community land model version 5: Description of new features, benchmarking, and impact of forcing uncertainty. *Journal of Advances in Modeling Earth Systems*, n/a.

Lewis, S.L., Malhi, Y. & Phillips, O.L. (2004). Fingerprinting the impacts of global change on tropical forests. *Philosophical Transactions of the Royal Society of London. Series B: Biological Sciences*, 359, 437–462.

Lines, E.R., Coomes, D.A. & Purves, D.W. (2010). Influences of forest structure, climate and species composition on tree mortality across the eastern US. *PLoS ONE*, 5, 1–12.

Martínez Cano, I., Muller-Landau, H.C., Wright, S.J., Bohlman, S.A. & Pacala, S.W. (2019). Tropical tree height and crown allometries for the barro colorado nature monument, panama: a comparison of alternative hierarchical models incorporating interspecific variation in relation to life history traits. *Biogeosciences*, 16, 847–862.

Massoud, E.C., Xu, C., Fisher, R.A., Knox, R.G., Walker, A.P., Serbin, S.P., Christoffersen, B.O., Holm, J.A., Kueppers, L.M., Ricciuto, D.M. *et al.* (2019). Identification of key parameters controlling demographically structured vegetation dynamics in a land surface model: Clm4. 5 (fates). *Geoscientific Model Development*, 12, 4133–4164.

McDowell, N., Allen, C.D., Anderson-Teixeira, K., Brando, P., Brienen, R., Chambers, J., Christoffersen, B., Davies, S., Doughty, C., Duque, A., Espirito-Santo, F., Fisher, R., Fontes, C.G., Galbraith, D., Goodsman, D., Grossiord, C., Hartmann, H., Holm, J., Johnson, D.J., Kassim, A.R., Keller, M., Koven, C., Kueppers, L., Kumagai, T., Malhi, Y., McMahon, S.M., Mencuccini, M., Meir, P., Moorcroft, P., Muller-Landau, H.C., Phillips, O.L., Powell, T., Sierra, C.A., Sperry, J., Warren, J., Xu, C. & Xu, X. (2018). Drivers and mechanisms of tree mortality in moist tropical forests. *New Phytologist*, 219, 851–869.

McDowell, N.G. & Allen, C.D. (2015). Darcy's law predicts widespread forest mortality under climate warming. *Nature Climate Change*, 5, 669–672.

McDowell, N.G., Beerling, D.J., Breshears, D.D., Fisher, R.A., Raffa, K.F. & Stitt, M. (2011). The interdependence of mechanisms underlying climate-driven vegetation mortality. *Trends in ecology & evolution*, 26, 523–532.

Mencuccini, M., Martínez-Vilalta, J., Hamid, H., Korakaki, E. & Vanderklein, D. (2007). Evidence for age-and size-mediated controls of tree growth from grafting studies. *Tree Physiology*, 27, 463–473.

Mencuccini, M., Martínez-Vilalta, J., Vanderklein, D., Hamid, H.A., Korakaki, E., Lee, S. & Michiels, B. (2005). Size-mediated ageing reduces vigour in trees. *Ecology Letters*, 8, 1183–1190.

Metcalf, C.J.E., Horvitz, C.C., Tuljapurkar, S. & Clark, D. (2009). A time to grow and a time to die: a new way to analyze the dynamics of size, light, age, and death of tropical trees. *Ecology*, 90, 2766–2778.

Moorcroft, P.R., Hurtt, G.C. & Pacala, S.W. (2001). A method for scaling vegetation dynamics: The ecosystem demography model (ed). *Ecological Monographs*, 71, 557–586.

Naito, Y., Kanzaki, M., Numata, S., Obayashi, K., Konuma, A., Nishimura, S., Ohta, S., Tsumura, Y., Okuda, T., Lee, S.L. & Muhammad, N. (2008). Size-related flowering and fecundity in the tropical canopy tree species, shorea acuminata (dipterocarpaceae) during two consecutive general flowerings. *Journal of Plant Research*, 121, 33–42.

Nepstad, D.C., Tohver, I.M., Ray, D., Moutinho, P. & Cardinot, G. (2007). Mortality of large trees and lianas following experimental drought in an amazon forest. *Ecology*, 88, 2259–2269.

Niklas, K.J. & Spatz, H.C. (2004). Growth and hydraulic (not mechanical) constraints govern the scaling of tree height and mass. *Proceedings of the National Academy of Sciences*, 101, 15661–15663.

Norby, R.J., Hanson, P.J., O'Neill, E.G., Tschaplinski, T.J., Weltzin, J.F., Hansen, R.A., Cheng, W., Wullschleger, S.D., Gunderson, C.A., Edwards, N.T. & Johnson, D.W. (2002). Net primary productivity of a co2-enriched deciduous forest and the implications for carbon storage. *Ecological Applications*, 12, 1261–1266.

O'Brien, S.T., Hubbell, S.P., Spiro, P., Condit, R. & Foster, R.B. (1995). Diameter, height, crown, and age relationship in eight neotropical tree species. *Ecology*, 76, 1926–1939.

Pachzelt, A., Forrest, M., Rammig, A., Higgins, S.I. & Hickler, T. (2015). Potential impact of large ungulate grazers on african vegetation, carbon storage and fire regimes. *Global Ecology and Biogeography*, 24, 991–1002.

Phillips, O.L., Aragão, L.E., Lewis, S.L., Fisher, J.B., Lloyd, J., López-González, G., Malhi, Y., Monteagudo, A., Peacock, J., Quesada, C.A. *et al.* (2009). Drought sensitivity of the amazon rainforest. *Science*, 323, 1344–1347.

Phillips, O.L., Vásquez Martínez, R., Arroyo, L., Baker, T.R., Killeen, T., Lewis, S.L., Malhi, Y., Monteagudo Mendoza, A., Neill, D., Núñez Vargas, P., Alexiades, M., Cerón, C., Di Fiore, A., Erwin, T., Jardim, A., Palacios, W., Saldias, M. & Vinceti, B. (2002). Increasing dominance of large lianas in amazonian forests. *Nature*, 418, 770–774.

Pugh, T.A.M., Rademacher, T.T., Shafer, S.L., Steinkamp, J., Barichivich, J., Beckage, B., Haverd, V., Harper, A., Heinke, J., Nishina, K., Rammig, A., Sato, H., Arneth, A., Hantson, S., Hickler, T., Kautz, M., Quesada, B., Smith, B. & Thonicke, K. (2020). Understanding the uncertainty in global forest carbon turnover. *Biogeosciences Discussions*, 2020, 1–44.

Purves, D.W., Lichstein, J.W., Strigul, N. & Pacala, S.W. (2008). Predicting and understanding forest dynamics using a simple tractable model. *Proceedings of the National Academy of Sciences*, 105, 17018–17022.

Read, J., Sanson, G.D., Jaffré, T. & Burd, M. (2006). Does Tree Size Influence Timing of Flowering in Cerberiopsis candelabra (Apocynaceae), a Long-Lived Monocarpic Rain-Forest Tree? *Journal of Tropical Ecology*, 22, 621–629.

Rüger, N., Huth, A., Hubbell, S.P. & Condit, R. (2011). Determinants of mortality across a tropical lowland rainforest community. *Oikos*, 120, 1047–1056.

Saldarriaga, J.G., West, D.C., Tharp, M.L. & Uhl, C. (1988). Long-term chronosequence of forest succession in the upper rio negro of colombia and venezuela. *Journal of Ecology*, 76, 938–958.

Sitch, S., Friedlingstein, P., Gruber, N., Jones, S.D., Murray-Tortarolo, G., Ahlström, A., Doney, S.C., Graven, H., Heinze, C., Huntingford, C., Levis, S., Levy, P.E., Lomas, M., Poulter, B., Viovy, N., Zaehle, S., Zeng, N., Arneth, A., Bonan, G., Bopp, L., Canadell, J.G., Chevallier, F., Ciais, P., Ellis, R., Gloor, M., Peylin, P., Piao, S.L., Le Quéré, C., Smith, B., Zhu, Z. & Myneni, R. (2015). Recent trends and drivers of regional sources and sinks of carbon dioxide. *Biogeosciences*, 12, 653–679.

Stephenson, N.L., Das, A.J., Condit, R., Russo, S.E., Baker, P.J., Beckman, N.G., Coomes, D.A., Lines, E.R., Morris, W.K., Rüger, N., Álvarez, E., Blundo, C., Bunyavejchewin, S., Chuyong, G., Davies, S.J., Duque, Á., Ewango, C.N., Flores, O., Franklin, J.F., Grau, H.R., Hao, Z., Harmon, M.E., Hubbell, S.P., Kenfack, D., Lin, Y., Makana, J.R., Malizia, A., Malizia, L.R., Pabst, R.J., Pongpattananurak, N., Su, S.H., Sun, I.F., Tan, S., Thomas, D., van Mantgem, P.J., Wang, X., Wiser, S.K. & Zavala, M.A. (2014). Rate of tree carbon accumulation increases continuously with tree size. *Nature*, 507, 90 EP –.

Stephenson, N.L., van Mantgem, P.J., Bunn, A.G., Bruner, H., Harmon, M.E., O'Connell, K.B., Urban, D.L. & Franklin, J.F. (2011). Causes and implications of the correlation between forest productivity and tree mortality rates. *Ecological Monographs*, 81, 527–555.

Terrer, C., Jackson, R.B., Prentice, I.C., Keenan, T.F., Kaiser, C., Vicca, S., Fisher, J.B., Reich, P.B., Stocker, B.D., Hungate, B.A., Peñuelas, J., McCallum, I., Soudzilovskaia, N.A., Cernusak, L.A., Talhelm, A.F., Van Sundert, K., Piao, S., Newton, P.C.D., Hovenden, M.J., Blumenthal, D.M., Liu, Y.Y., Müller, C., Winter, K., Field, C.B., Viechtbauer, W., Van Lissa, C.J., Hoosbeek, M.R., Watanabe, M., Koike, T., Leshyk, V.O., Polley, H.W. & Franklin, O. (2019). Nitrogen and phosphorus constrain the co2 fertilization of global plant biomass. *Nature Climate Change*, 9, 684–689.

Vilalta, J.M. (2005). Size, not cellular senescence, explains reduced vigour in tall trees. *Ecology Letters*, 8, 1183–1190.

Walker, A.P., Zaehle, S., Medlyn, B.E., De Kauwe, M.G., Asao, S., Hickler, T., Parton, W., Ricciuto, D.M., Wang, Y.P., Warlind, D. & Norby, R.J. (2015). Predicting long-term carbon sequestration in response to co2 enrichment: How and why do current ecosystem models differ? *Global Biogeochemical Cycles*, 29, 476–495.

Wang, L., Cui, J., Jin, B., Zhao, J., Xu, H., Lu, Z., Li, W., Li, X., Li, L., Liang, E., Rao, X., Wang, S., Fu, C., Cao, F., Dixon, R.A. & Lin, J. (2020). Multifeature analyses of vascular cambial cells reveal longevity mechanisms in old ginkgo biloba trees. *Proceedings of the National Academy of Sciences*.

Wheelwright, N.T. & Logan, B.A. (2004). Previous-year reproduction reduces photosynthetic capacity and slows lifetime growth in females of a neotropical tree. *Proceedings of the National Academy of Sciences*, 101, 8051–8055.

Wright, S., Kitajima, K., Kraft, N., Reich, P., Wright, I., Bunker, D., Condit, R., Dalling, J., Davies, S., Díaz, S., Engelbrecht, B., Harms, K., Hubbell, S., Marks, C., Ruiz-Jaen, M., Salvador, C. & Zanne, A.E. (2010). Functional traits and the growth-mortality trade-off in tropical trees. *Ecology*, 91, 3664–3674.

Yanoviak, S.P., Gora, E.M., Fredley, J., Bitzer, P.M., Muzika, R.M. & Carson, W.P. (2015). Direct effects of lightning in temperate forests: a review and preliminary survey in a hemlock–hardwood forest of the northern united states. *Canadian Journal of Forest Research*, 45, 1258–1268.

Yap, S.L., Davies, S.J. & Condit, R. (2016). Dynamic response of a philippine dipterocarp forest to typhoon disturbance. *Journal of Vegetation Science*, 27, 133–143.

Yu, K., Smith, W.K., Trugman, A.T., Condit, R., Hubbell, S.P., Sardans, J., Peng, C., Zhu, K., Peñuelas, J., Cailleret, M., Levanic, T., Gessler, A., Schaub, M., Ferretti, M. & Anderegg, W.R.L. (2019). Pervasive decreases in living vegetation carbon turnover time across forest climate zones. *Proceedings of the National Academy of Sciences*.

Zaehle, S., Medlyn, B.E., Kauwe, M.G.D., Walker, A.P., Dietze, M.C., Hickler, T., Luo, Y., Wang, Y., El-Masri, B., Thornton, P., Jain, A., Wang, S., Warlind, D., Weng, E., Parton, W., Iversen, C.M., Gallet-Budynek, A., McCarthy, H., Finzi, A., Hanson, P.J., Prentice,

I.C., Oren, R. & Norby, R.J. (2014). Evaluation of 11 terrestrial carbon–nitrogen cycle models against observations from two temperate free-air co2 enrichment studies. *New Phytologist*, 202, 803–822.

Zhu, Z., Piao, S., Myneni, R.B., Huang, M., Zeng, Z., Canadell, J.G., Ciais, P., Sitch, S., Friedlingstein, P., Arneth, A., Cao, C., Cheng, L., Kato, E., Koven, C., Li, Y., Lian, X., Liu, Y., Liu, R., Mao, J., Pan, Y., Peng, S., Peñuelas, J., Poulter, B., Pugh, T.A.M., Stocker, B.D., Viovy, N., Wang, X., Wang, Y., Xiao, Z., Yang, H., Zaehle, S. & Zeng, N. (2016). Greening of the earth and its drivers. *Nature Climate Change*, 6, 791–795.
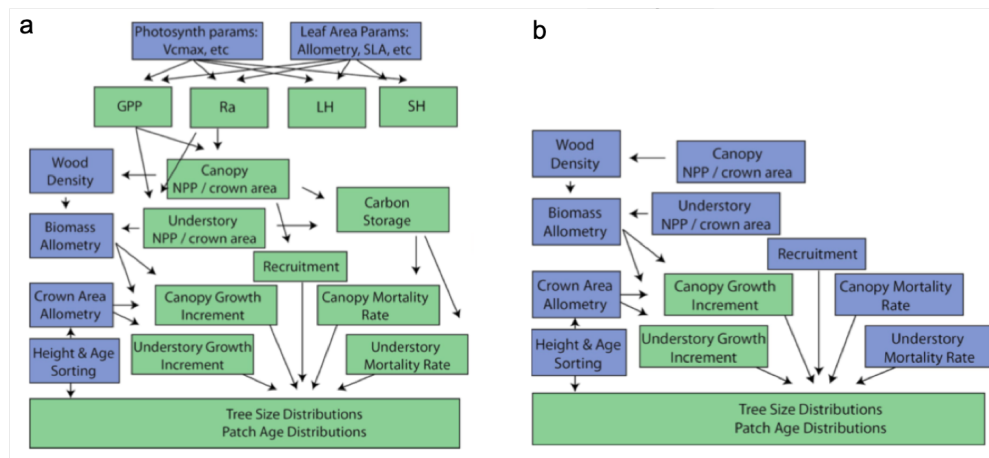
9 Figures

Figure 1: Schematic of "prescribed physiology mode" in FATES. Blue boxes show model parameters, green boxes show model predictions. a) shows the full model where recruitment, NPP and mortality are emergent properties of physiological pathways and functional trait values. b) shows prescribed physiology mode where recruitment, NPP and mortality become model parameters. Prescribed physiology mode enables direct tests of the impact of demographic rates on model outcomes at both the individual and carbon scale.
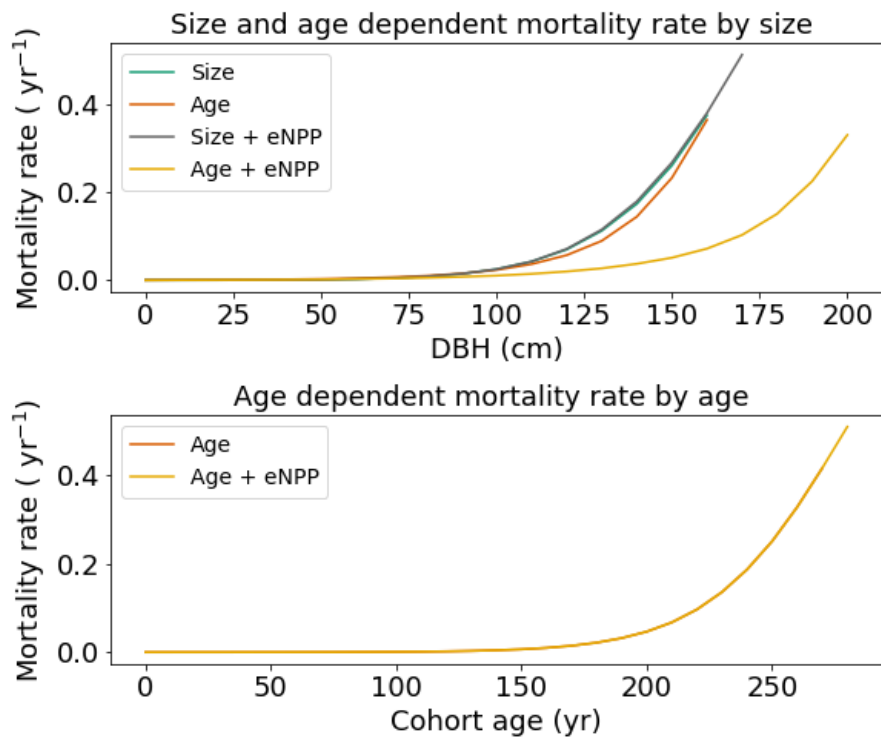
Figure 2: Size and age dependent mortality rates, with and without eNPP. Size-dependent mortality does not change with an increase in NPP, whereas age-dependent mortality is shifted to larger sizes (top panel) with no change to the age-dependency (lower panel).
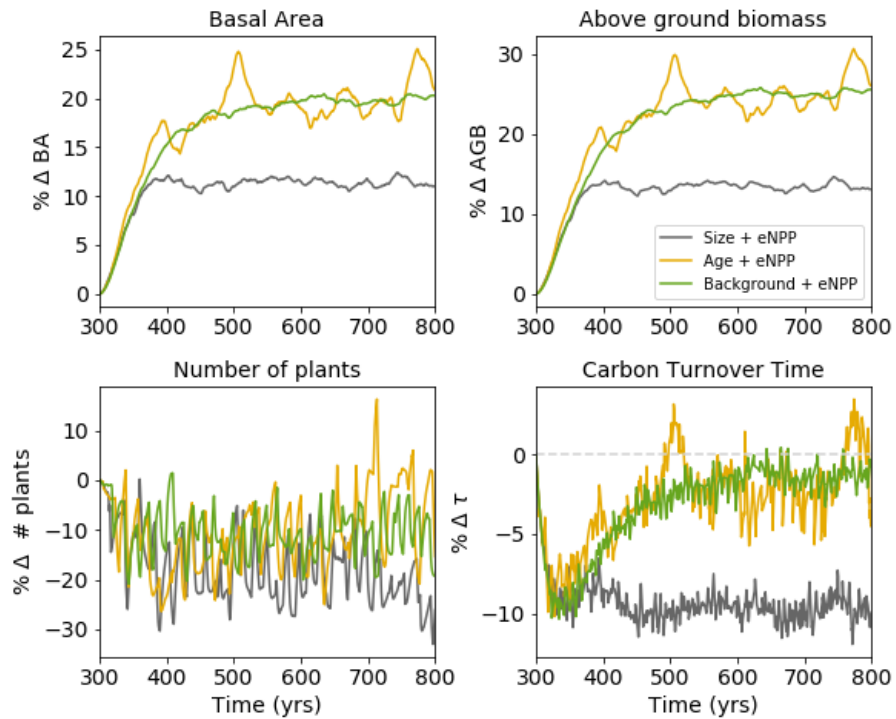
Figure 3: Change in basal area (BA), aboveground biomass (AGB), number of individuals, and carbon turnover time (τ) of background, size- and age-dependent mortality simulations following simulated eNPP. The y axis in all panels is the percent change under eNPP relative to constant NPP. Note the x axes begin in year 300, the point at which the simulated increase in eNPP begins. AGB and BA increases were greater when mortality was just background or age-dependent. The decrease in τ was greatest when mortality was size-dependent.
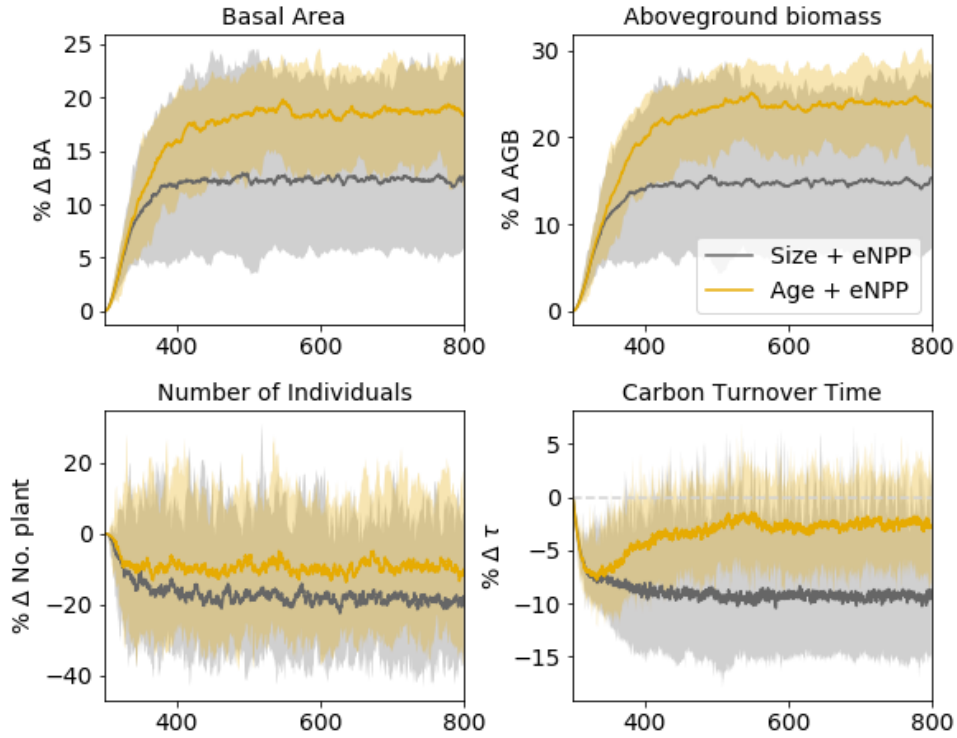
Figure 4: Change in aboveground biomass (AGB), basal area (BA), number of individuals and carbon turnover time (τ) following eNPP in two PFT size- and age-dependent mortality scenarios. Solid lines show the median and shading the 95th percentile from ensemble runs. AGB and BA increase with both types of mortality, but more so with age-dependent mortality. τ decreases with both size- and age-dependent mortality but more so with size-dependent mortality. Demographic differences between ensemble members led to wide variation in forest response to eNPP.
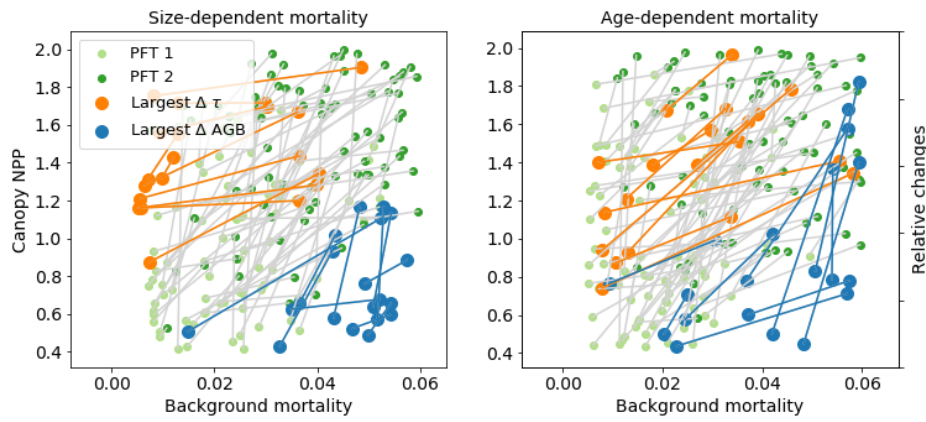
Figure 5: Position of all PFT pairs in parameter space, and the position of pairs that showed the greatest relative reduction in carbon turnover time (τ), or increase in AGB following eNPP, with both size-dependent (left) and age-dependent mortality (right). In both mortality scenarios, the change in τ was greatest when background mortality was low and canopy NPP was high. With low background mortality a greater proportion of cohorts survive to reach either the size or age at which size- or age-dependent mortality takes effect, and hence there is a greater relative speeding up of the life cycle (size-dependent mortality), or increased demotion of cohorts to the canopy due to increased sizes (age-dependent mortality). Higher NPP amplifies these effects. The greatest increase in AGB in both mortality scenarios was when background mortality was high and NPP low, as these PFT pairs had low initial AGB and saw the largest relative increase in AGB following a 25% increase in NPP.
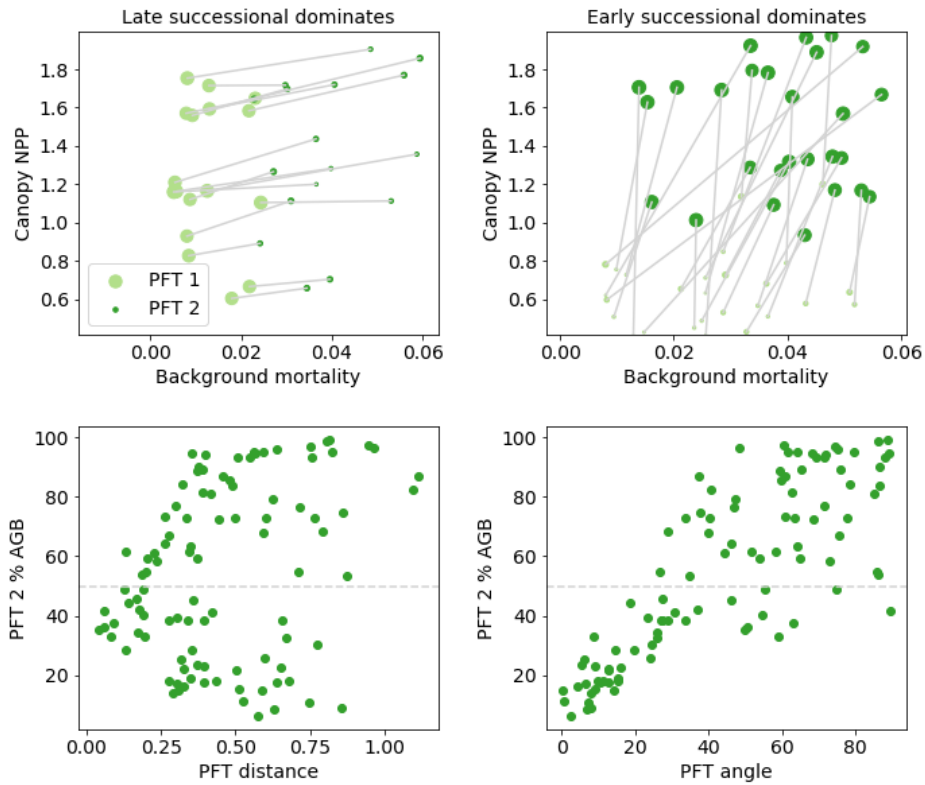
Figure 6: Coexistence of PFT pairs. Top panels show the position of PFT pairs in parameter space where the late successional PFT (PFT 1) (left) or early succesional PFT (PFT 2) (right) makes up greater than 80% of plot AGB (prior to eNPP). Bottom panels show the percentage of plot AGB in the early successional PFT against the angle and distance between PFTs in each pair. Early successional PFTs dominate when the difference in NPP between PFTs is greater than the difference in mortality (high angle) (top right, bottom right). Late successional PFTs dominate when differneces in mortality are large relative to differences in NPP between PFT pairs (small angles) (top left, bottom right). PFTs are more equal when the demographic distance between them is small (bottom left). As they become more demographically different one or the other starts to dominate AGB. These results are for size-dependent mortality but results were similar for age-dependent mortality (see Fig. S3).
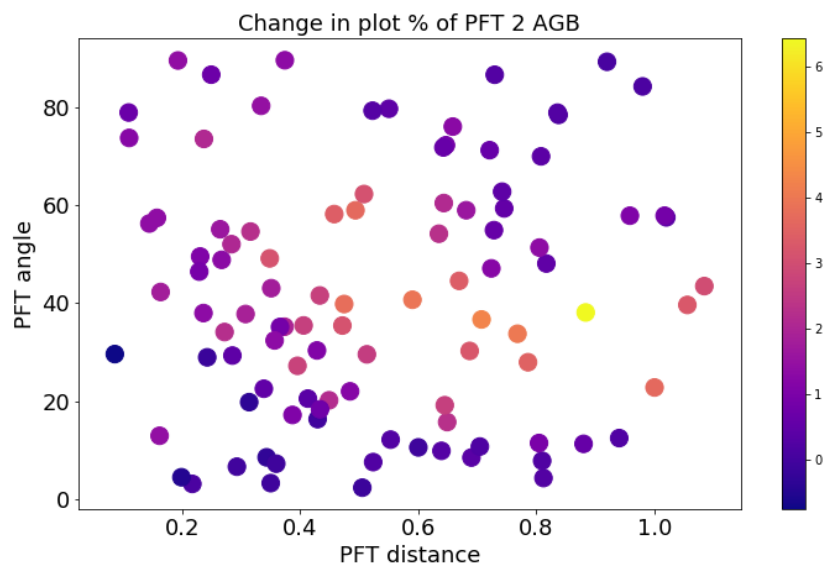
Figure 7: Change in the percent AGB of the early successional PFT (PFT 2) following the increase in NPP. The early successional PFT was able to increase most following simulated eNPP when the distance between PFT pairs was intermediate and the angle between PFT pairs was low. The early successional PFT decreased in plot AGB when the angle between PFTs was high. These results are for age-dependent mortality but results were similar with size-dependent mortality (see Fig. S4).